Corrosion Performance of Laser Posttreated Cold Sprayed Titanium Coatings

T. Marrocco, T. Hussain, D.G. McCartney, and P.H. Shipway

(Submitted November 29, 2010; in revised form February 14, 2011)

The recent development of cold spray technology has made possible the deposition of highly reactive, oxygen sensitive materials, such as titanium, without significant chemical reaction of the powder, modification of particle microstructure and with minimal heating of the substrate. However, the presence of interconnected pathways (microscale porosity) within the deposit limits the performance of the metallic coating as an effective barrier to corrosion and substrate attack by corrosive media is usually inevitable. The aim of the present study was to investigate the effects of processing, including a postspray laser treatment, on the deposit microstructure and corrosion behavior. Commercially pure titanium (CP Ti) was deposited onto a carbon steel substrate, using a commercial cold spray system (CGT^{TM} Kinetiks$^{®}$ 4000) with preheated nitrogen as both the main process gas and the powder carrier gas. Selected coatings were given a surface melting treatment using a commercial 2 kW CO_2 laser (505 Trumpf DMD). The effect of postdeposition laser treatment on corrosion behavior was analyzed in terms of pore structure evolution and microstructural changes. Optical microscopy, scanning electron microscopy, and x-ray diffraction were employed to examine the microstructural characteristics of the coatings. Their corrosion performance was investigated using electrochemical methods in 3.5 wt.% NaCl (ASTM G5-94 (2004)). As-sprayed titanium coatings could not provide favorable protection to the carbon steel substrate in the aerated NaCl solution, whereas the coatings with laser-treated surfaces provided barrier-like properties.

Keywords	cold spray, corrosion, laser treatment, titanium

1. Introduction

Thanks to their many unique characteristics, titanium and its alloys perform very well (as few other materials can) in many challenging environments, such as aerospace, petrochemical, marine, bio-implants, and motorsports (Ref 1). The outstanding resistance to corrosion in a wide range of aggressive media is a result of a tenacious protective oxide layer (TiO_2), which is always present because of the high affinity of titanium for oxygen and water vapor. The oxide film is sufficiently thick to passivate the metal and is quickly reestablished when locally destroyed, e.g., by mechanical action (Ref 2). With the high price of corrosion resistant materials (such as titanium and its alloys) in bulk form, there are major financial incentives to use Ti-coated, lower cost substrates. Increasing attention has been paid to the spraying of titanium with the deposited coatings designed to be used for protection of substrates, particularly, in aqueous environments where electrochemical corrosion can occur (Ref 3).

Thermal spraying (typically flame or plasma spraying) of reactive materials such as titanium can cause a considerable change in chemical composition from powder to coating, which should be minimized as far as possible. During spraying, gas adsorption onto particles from the atmosphere, decomposition, phase changes, and oxidation or nitridation of the spray particles can occur in ways that may be difficult to control (Ref 4). In addition, oxidation of spray particles after impact is also potentially significant due to their exposure to the atmosphere with an increased surface area produced by deformation (flattening) while still hot and during the cooling period. In some applications (e.g., biotechnology), phase purity is of utmost importance, and oxidation or phase changes that occur during the spray operation can lead to total rejection of the sprayed coating. If interactions between the molten particles and the reactive gas molecules are detrimental to the properties and the particular application, spraying in a vacuum chamber has been, hitherto, the main alternative (Ref 5).

On the other hand, cold spray, as a solid state process, permits deposition of titanium coatings under open atmospheric conditions without significant reaction (with oxygen or nitrogen) and with generally low porosity. The process involves the acceleration of fine powders to 500-1000 m/s in a supersonic inert gas jet. On impact with the target surface, the solid particles experience high-strain rate deformation, forming a bond with the substrate and each other to produce a low porosity and well-adhered coating (Ref 6). The technology has now reached a significant stage in its industrialization, with proven commercial equipment now available, together with suppliers

T. Marrocco, TWI Ltd, Granta Park, Great Abington, Cambridge, UK; and **T. Hussain**, **D.G. McCartney**, and **P.H. Shipway**, School of Mechanical, Materials and Manufacturing Engineering, University of Nottingham, University Park, Nottingham, UK. Contact e-mail: tiziana.marrocco@twi.co.uk.

offering specially developed powders to ensure good coating quality. Specifically, absence of porosity in cold sprayed titanium coatings plays a critical role in forming a corrosion resistant barrier layer. The type of gas used as the main process gas has a strong influence on the porosity of the coatings (Ref 7-9). In general, a less porous coating structure has been observed when helium is used as the accelerating gas (compared to coatings sprayed with nitrogen) because the particle velocity is greatly increased under the same operating conditions due to the higher specific heat and lower molecular weight of helium (Ref 10). Evidence of this can be found in the study carried out by Li and Li (Ref 11), which reveals formation of large pores open to the surface when titanium coatings were cold sprayed using nitrogen as the propellant gas.

Hence, attack of substrates which are not corrosion resistant by corrosive media is usually inevitable as reported in detail by the present authors in Ref 12. In Ref 12, it is shown that deposits sprayed with heated nitrogen gas onto carbon steel substrates could be produced with a total interconnected porosity of 5.9 vol.% such that 4.5 vol.% was below 1 μm with the balance above 1 μm in size. These measurements were obtained using mercury intrusion porosimetry. It was also shown (Ref 12) that these deposits did not provide an impermeable barrier. The corrosion performance of titanium (cold sprayed onto carbon steel substrate and bulk titanium) in natural seawater was also studied by Wang et al. (Ref 13) by using open circuit potential (OCP) measurements and potentiodynamic polarization. They reported that the OCP of cold sprayed titanium was more negative than the bulk titanium due to the high surface activity (of the top layer of the deposit) and limited bonding at the inter-particle boundaries. Similarly arc, flame, atmospheric plasma sprayed (shrouded), and warm-sprayed titanium coatings show a higher corrosion current density compared to bulk titanium due to the presence of oxides, nitrides and most importantly porosity (Ref 14-17).

Laser processing is used in surface engineering for melting, cladding, alloying, and transformation hardening of materials (Ref 18). Typically, the very high power density of laser beam ($\sim 10^{10-12} \text{W/m}^2$) provides deep penetration. However, in the case of surface engineering applications, the beam is usually defocused to reduce penetration and increase coverage rate (i.e., it is possible to melt the coating while the substrate can remain virtu-

ally unaffected). In laser surface melting, the heat energy from the laser beam is sufficient to melt the surface without vaporizing the material. A melt pool is formed at the material surface which is governed by the forces of buoyancy due to density difference and convection due to surface tension gradients. The bulk material acts as a heat sink and as soon as the laser beam traverses past, the solidification process starts from the solid-liquid interface toward the surface (Ref 19). Laser melting of the coating promotes a homogeneous and refined microstructure as a result of rapid melting and solidification which potentially can improve corrosion properties. A number of postspray treatments (e.g., laser surface melting and electron beam diffusion) have been reported to improve the corrosion behavior of plasma-sprayed titanium coatings (Ref 1, 16, 20). The laser-consolidated coating showed no evidence of corrosion after testing for 15 days, whereas the coating left in the as-sprayed condition showed pitting corrosion of the steel at the coating-steel substrate interface (Ref 20).

The current study investigated the effects of a postspray laser treatment performed on titanium coatings that were cold sprayed onto a carbon steel substrate. The microstructural characterization and porosity measurements (using mercury intrusion porosimetry) of the cold sprayed titanium coatings are extensively detailed in a previous publication by the authors (Ref 12). In the present study, selected coatings from that original work were given a surface melting treatment using a 2 kW Trumpf DMD 505 CO_2 laser and their microstructure and corrosion behavior investigated. Optical microscopy, scanning electron microscopy, and x-ray diffraction were employed to examine the microstructural characteristics of the coatings. Their corrosion performance was investigated using electrochemical methods in 3.5 wt.% NaCl (ASTM G5-94 (2004)).

2. Experimental Methods

2.1 Materials

Commercially pure gas-atomized titanium powder (LPW, Cheshire, UK) was used to produce the deposits. Details of the chemistry and nominal particle size distribution, as provided by the powder manufacturer, are reported in Table 1. The feedstock powder was spherical

Table 1 Chemical composition and particle size distribution of the titanium powder as supplied by the manufacturer and size distribution measured by laser diffractometry

Powder	Chemical composition, wt.%					
CP-Ti grade 2	C	Fe	H	N	O	Ti
	0.008	0.057	0.002	0.002	0.200	Bal.
	Particle size distribution, μm					
				D_{10}	D_{50}	D_{90}
Supplied				7	16	27
Measured				10	15	20

in shape with only a very small fraction exhibiting satellite particles, as expected for gas-atomized powders (Fig. 1a). The particle size distribution of the feedstock powder was measured using laser diffractometry (Table 1). The particle size analysis measured by laser diffractometry showed that 90% of the particles were in the supplier specified size range of $-30 + 10$ μm with approximately 10 vol.% below 10 μm (Fig. 1b).

All coatings were deposited onto grit-blasted carbon steel (BS 970-1:1983 Grade 045M10) substrates of dimension $40 \times 25 \times 2$ mm. All substrates were ultrasonically cleaned in acetone prior to use and given a final clean using acetone to remove any surface residue introduced while mounting the samples for spraying.

2.2 Spraying Procedure

All coatings were deposited at TWI using a CGT Kinetiks 4000/47® cold spray system. The system is capable of spraying at gas pressures and temperatures of 40 bar and 800 °C, respectively. The spray gun was mounted on a six-axis robot to allow accurate control of the spraying pattern and used with a de Laval nozzle with an area expansion ratio of ~6.5. In all cases, the coatings were deposited using oxygen-free nitrogen (OFN ≤ 5 ppm O_2, <8 ppm H_2O) as both the main process and carrier gas. The main spray parameters used are shown in Table 2. Scanning the spraying gun over the coupons for a total of
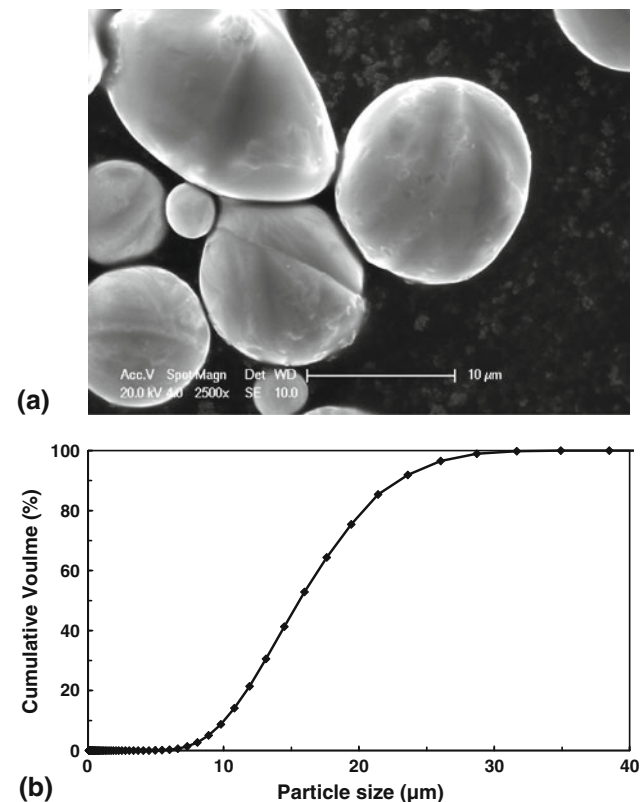

(a)

(b)

Fig. 1 (a) Scanning electron micrograph of gas-atomized grade 2 titanium feedstock powder. (b) Cumulative size distribution of titanium powder measured by laser diffractometry

three passes, a coating thickness of ~500-600 μm was achieved.

2.3 Postspray Laser Treatment

Following coating deposition, samples were laser treated using a Trumpf DMD 505 (Trumpf GmbH, Ditzingen, Germany) 2 kW CO_2 laser. The laser was used to melt only the top layer of the material in a protective helium atmosphere to prevent, as far as possible, oxidation of titanium. The samples were clamped on a copper block to dissipate the heat produced from the laser heating and avoid distortion of the substrates and coatings and the possibility of delamination. The trials were carried out with laser power ranging from 440 to 1000 W, a traverse speed of 21.6-48.3 mm/s and a beam diameter of 0.3-1.08 mm measured using a Prometec beam profiler (Prometec GmbH, Aachen, Germany).

A rectangular laser-treated area (16×16 mm) was prepared on each of the cold sprayed titanium coatings (40×25 mm), using overlapping tracks. A number of preliminary trials were conducted to assess the appropriate conditions to achieve surface melting without delamination and study the shape and depth of melt pool. Five different laser process conditions were employed, as listed in Table 3; Run 3 parameters were used to produce the laser-treated areas that were subjected to corrosion testing.

2.4 Microstructural Characterization of Coatings

A metallographic cross section was prepared from each coating by cutting samples with a diamond slitting wheel. To remove any effects associated with cutting the specimen, following mounting, the sample was ground back ~2 mm using P120 (125 μm) grit silicon carbide (SiC) paper. Progressive grinding with finer grades was carried out, finishing with P1200 (15.3 μm) grit SiC paper. This was followed by polishing with successively finer diamond pastes and then a final polishing using a 10:1 solution of suspended colloidal (0.1 μm) silica solution and H_2O_2 on a MD-Chem cloth (Struers UK). The prepared sections were examined using optical and scanning electron microscopy. An FEI XL30 (FEI Europe, Eindhoven, The Netherlands) scanning electron microscope (SEM) operating at 20 kV was employed to examine the microstructures of the coatings. The coatings were lightly etched in Kroll's etchant (2% HF, 5% HNO_3, and 95% H_2O) for a standard time of 15 s prior to examination in the microscope.

Table 2 Process parameters used for depositing the titanium coating with the CGT Kinetiks 4000/47® system

Process parameter	Set value
P_{GAS}, bar (MPa)	40 (4.0)
GFR, m³/h (l/min)	80 (1333)
T_{GAS}, °C	800
PFR, g/min (kg/h)	27 (1.6)
SOD, mm	40

P_{GAS} is the gas pressure, GFR is the total nitrogen gas flow rate, PFR is the measured powder feed rate, and SOD is the stand-off distance

Table 3   Process parameters for single track runs in the laser surface treatment of the titanium coatings

Run No	Power (P), W	Scanning speed (V), mm/s	Spot size (D), mm	Track (melt) width, μm	Melted depth, μm	$\frac{P}{\sqrt{D \times V}}$, N/√s (E+05)
1	440	25	0.3	500	110	1.61
2	540	25	0.408	600	130	1.69
3	1000	21.6	0.108	1200	140	2.07
4	1000	31.6	0.108	1200	115	1.71
5	1000	48.3	0.108	1200	55	1.38

Run #3 parameters were employed in the final treatment of the corrosion test samples

To determine the phases present in each coating both before and after laser treatment, x-ray diffraction was performed on the top surface using a Siemens D500 diffractometer (Siemens Analytics, Munich, Germany). This was operated at 40 kV and 25 mA to generate monochromatic Cu K_α radiation with a wavelength of 0.15406 nm. A 2θ diffraction angle ranging from 30° to 90° was employed with a dwell time of 5 s per step and a step size 0.05°. Phases present in the spectra were identified with the aid of Joint Committee on Powder Diffraction Standards (JCPDS) diffraction files. Scans of the coatings were performed on 10 × 10 mm² samples mounted on a suitable holder.

2.5 Corrosion Testing

To determine whether the titanium coating was resistant to chloride attack and whether it produced a physical barrier (i.e., no interconnected porosity) for the steel substrate, electrochemical studies were conducted on the coating in the as-sprayed and postlaser-treated conditions, using an ACM Gill 8 sequencer (ACM Instruments, Cumbria, UK). The samples were prepared to a P1200 (15.3 μm) grit surface finish. The coatings were tested in a standard three-electrode cell at 30 °C and in aerated 3.5 wt.% NaCl aqueous solution. The OCP of the specimens was measured for the first 60 min of immersion before starting the potentiodynamic scans. To conduct the anodic scans, samples were first lowered to a potential 200 mV below the open circuit value and then scanned in the anodic direction at a rate of 20 mV/min. All the potentials were measured with respect to an Ag/AgCl reference electrode and a platinum plate was used as a counter electrode.

3. Results

Initially, to allow the most suitable selection of parameters, the laser was scanned over the cold sprayed titanium coatings in a single pass and metallographic cross sections were prepared from all the tracks to analyze the shape and depth of the melt pool as shown in the optical micrographs of Fig. 2. In all cases, the laser-treated regions are seen to comprise pore-free regions with equiaxed grains; making them easily distinguishable from the unmelted as-sprayed region featuring inter-particle porosity. The densification of the laser-treated region is

due to its melting and porosity escaping to the free surface with the subsequent resolidification of the treated area. An empirical relationship between power density parameters $(P/(DV)^{1/2}$, where P is the laser power, D is the spot diameter, and V is the scanning traverse speed) and the melting depth was reported by Steen (Ref 18). The relationship between this parameter and melted depth and width determined in the present study is shown in Table 3. From Run 3 to Run 5, the beam diameter was fixed at 1080 μm and an increase of the $P/(DV)^{1/2}$ value correlates with a decrease of the melting depth. Increasing the power (P) increases the depth and width of the melted region by 20 and 100 μm, respectively (Fig. 2a and b) whereas, as the traverse speed (V) increases, the melted depth decreases but with less change in track width (Fig. 2c-e). Values of depth and width of the melting regions are shown in Table 3.

On the basis of these single tracks, Run 3, which had the highest $P/(DV)^{1/2}$ value, was selected to treat an area of 16 × 16 mm. Overlapping track trials were performed using a range of track off-sets from 200 to 1000 μm. Eventually, an off-set of 1000 μm was used, resulting in a track overlap of only 200 μm. The back-scattered electron (BSE) image of the etched cross section of the laser-treated coating is shown in Fig. 3(a). Here, the depth of the laser melt pool can be identified as the point at which inter-particle pores of the titanium coating begin. It can be seen that, at the center of the melt pool, the penetration depth is ~140 μm whereas at the edge (i.e., where two laser tracks were overlapped) is about ~100 μm. Nevertheless, the parameters of Run 3 (Table 3) sealed the coating top surface uniformly and without any gaps. The high magnification, secondary electron (SE) image of the laser-treated area (Fig. 3b) reveals the acicular microstructure of titanium and isolated rounded pores (marked with arrows).

Figure 4 shows x-ray diffraction patterns of both the as-sprayed coating and the laser-treated coating. Clearly, the main phase present in both cases is seen to be α-Ti. The pattern from the as-sprayed coating does not show any evidence for oxides or nitrides within the limits of XRD sensitivity (i.e., 1-2 wt.%). However, for the laser-treated coating, small peaks corresponding to TiO (Hongquiite) are seen at 2θ angles of 36°, 42°, and 61°. This is evidence for some limited oxidation occurring during laser melting due to the high reactivity of titanium, despite the fact that the laser treatment was conducted in a protective helium atmosphere. The other feature of note
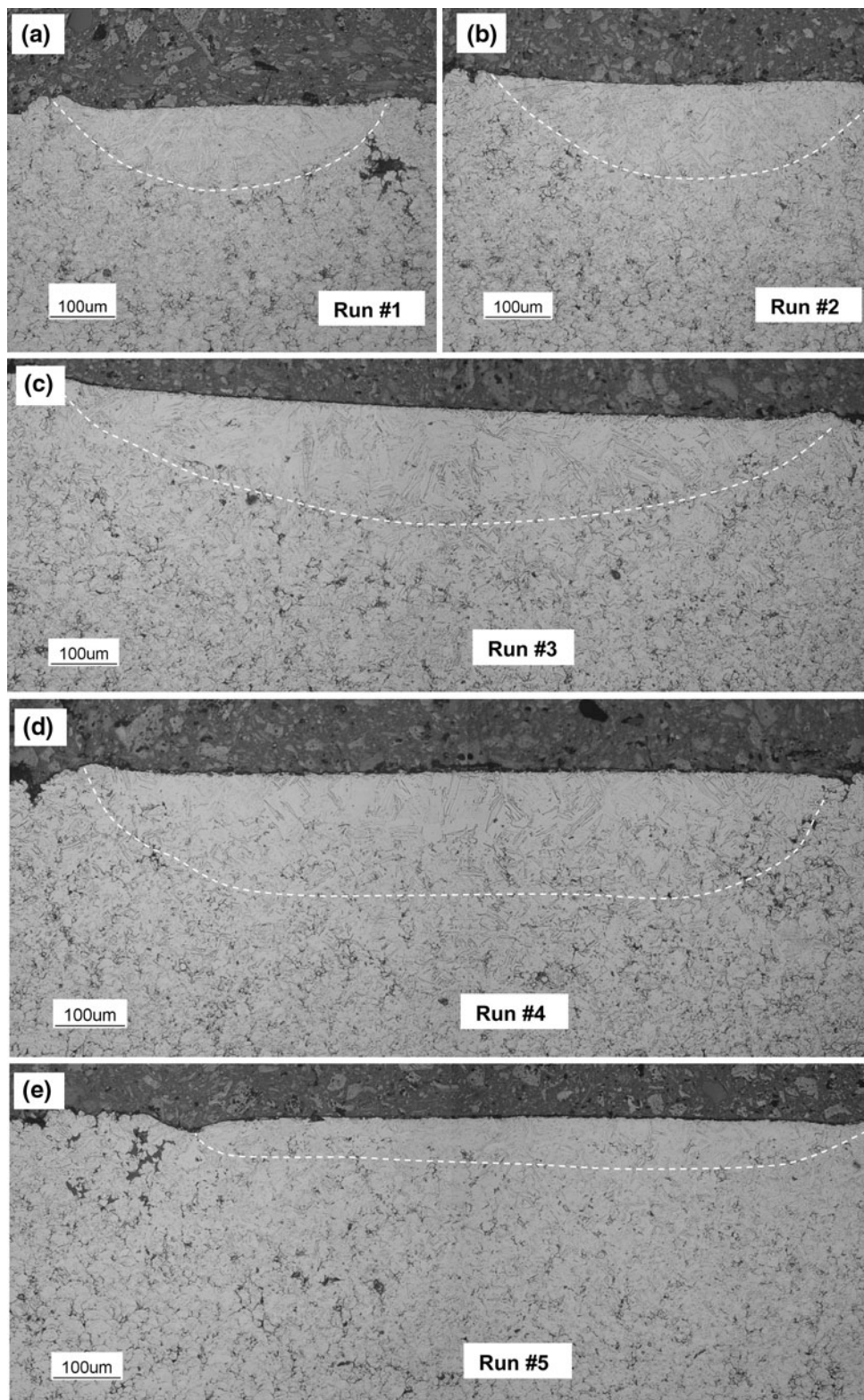
Fig. 2 Optical micrographs showing laser-treated areas in titanium coatings, Runs 1-5. All cross sections were etched prior to microscopy
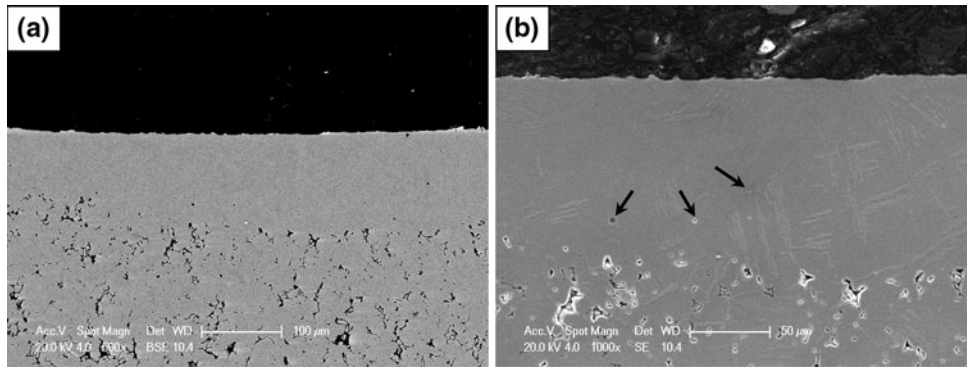
Fig. 3 (a) Back scattered electron (BSE) image of a laser-treated titanium coating showing the shape of the melt pool and (b) secondary electron (SE) image showing the microstructure of the laser-treated zone. Both cross sections were taken from the coating treated in Run 3 and etched in Kroll's reagent prior to microscopy. Arrows showing isolated pores
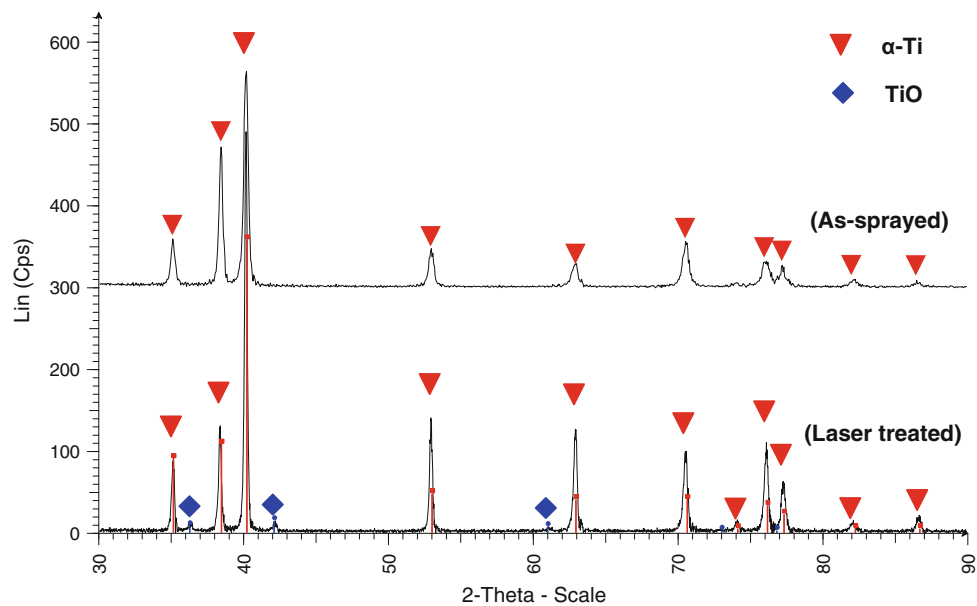

Fig. 4 X-ray diffraction spectra of the as-sprayed and laser-treated titanium coating (Run 3)

is the evident peak broadening in the spectrum from the as-sprayed sample. This can, presumably, be attributed to the high degree of microstrain and/or submicron coherent diffracting domain size arising from the high strain rate impact of powder particles.

Figure 5 shows the OCP values of bulk titanium, carbon steel, as-sprayed coating (on carbon steel), and a laser-treated coating (on carbon steel) in aerated solution for 3600 s. The OCP of bulk titanium increased steadily over the period of the experiment and reached approximately −285 mV from an initial value of −600 mV. This change could be due to the growth and establishment of a more protective surface oxide film on the initially as-ground Ti surface when exposed to the test solution (Ref 23). However, the reasons for the noise on the bulk Ti curve are not presently understood but could be due to localized and repeated corrosion events on the surface during the establishment of the more stable oxide. In contrast, the

as-sprayed titanium coating had a much lower steady state OCP of about −500 mV and remained at that level during the full length of the experiment. The laser-treated titanium coating, on the other hand, showed a relatively steady OCP which reached about −285 mV; the same as that of bulk titanium after 3600 s. The fact that it did not increase over time like bulk Ti would suggest it already had a stable oxide film on its surface prior to immersion or that it formed within the first few second of immersion. This could be due to the presence of the TiO phase noted to be present from the XRD pattern of Fig. 4. Therefore, the laser treatment of the coating shifted the OCP by about −210 mV in the more positive direction (i.e., toward the value of bulk titanium) compared to the as-sprayed titanium coating. The steady decrease in the OCP exhibited by bulk carbon steel from −400 to −600 mV was indicative of ongoing active corrosion experienced by the ground steel specimen in the test solution. It is also notable that the
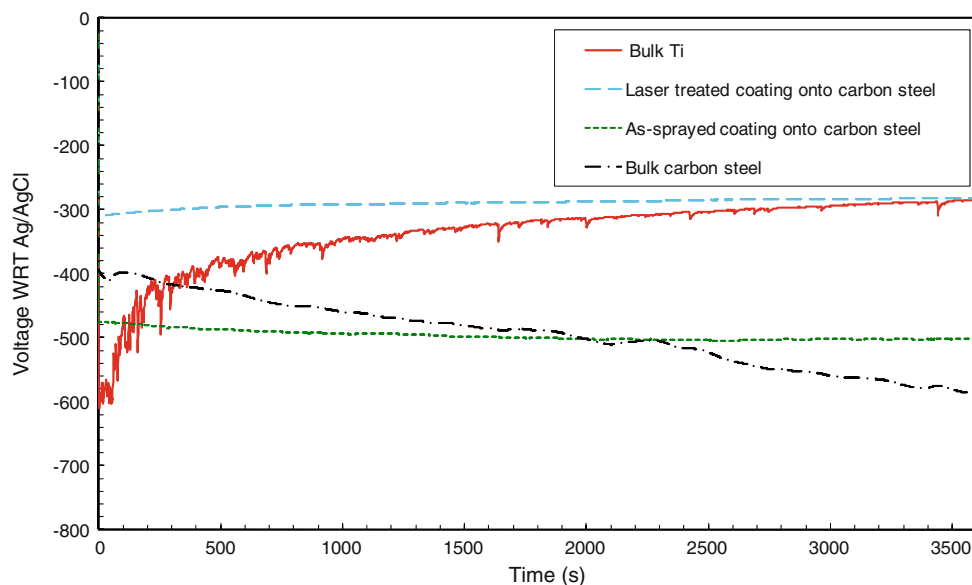
Fig. 5 Open circuit potential (OCP) in aerated 3.5% NaCl of bulk Ti, carbon steel, as-sprayed Ti coating (on carbon steel), and laser-treated Ti coating
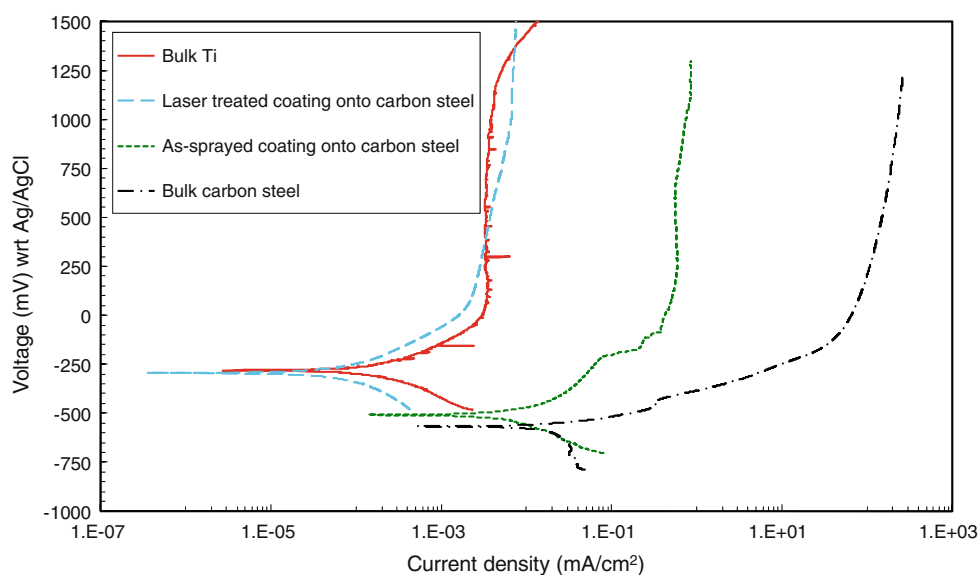

Fig. 6 Potentiodynamic polarization scans in aerated 3.5% NaCl of bulk Ti, carbon steel, as-sprayed Ti coating (on carbon steel), and laser-treated Ti coating

OCP of the as-sprayed coating attained a value between bulk Ti and bulk carbon steel which is indicative of a porous microstructure.

Potentiodynamic polarization scans of bulk titanium, carbon steel, the as-sprayed coating (on carbon steel), and the laser-treated coating (on carbon steel) are shown in Fig. 6. Bulk titanium shows a passive current density (I_{pp}) of 0.004 mA/cm^2, whereas the as-sprayed titanium coating shows only a "passive like" current density of 0.6 mA/cm^2, which is two orders of magnitude greater than that of bulk titanium. However, the laser-treated coating shows an average I_{pp} of 0.005 mA/cm^2, which is virtually the same as

the bulk titanium and two orders of magnitude lower than that of the as-sprayed coating. Occasional spikes seen on the anodic polarization curve of the bulk Ti could be due to isolated pitting and re-passivation events as the voltage is increased. In addition, the as-sprayed coating had an I_{corr} value of 5×10^{-3} mA/cm^2; which was reduced to 5×10^{-5} mA/cm^2 following laser treatment (Table 4). E_{corr} values of all the samples showed a similar trend to the OCP measurements. A number of small current transients were observed in the bulk Ti scan which may be attributed to metastable pitting during establishment of a more protective surface oxide film on the ground Ti surface.

Table 4 Corrosion values (in aerated 3.5 wt.% NaCl) of bulk titanium, as-sprayed coating (on carbon steel), laser-treated coating, and bulk carbon steel

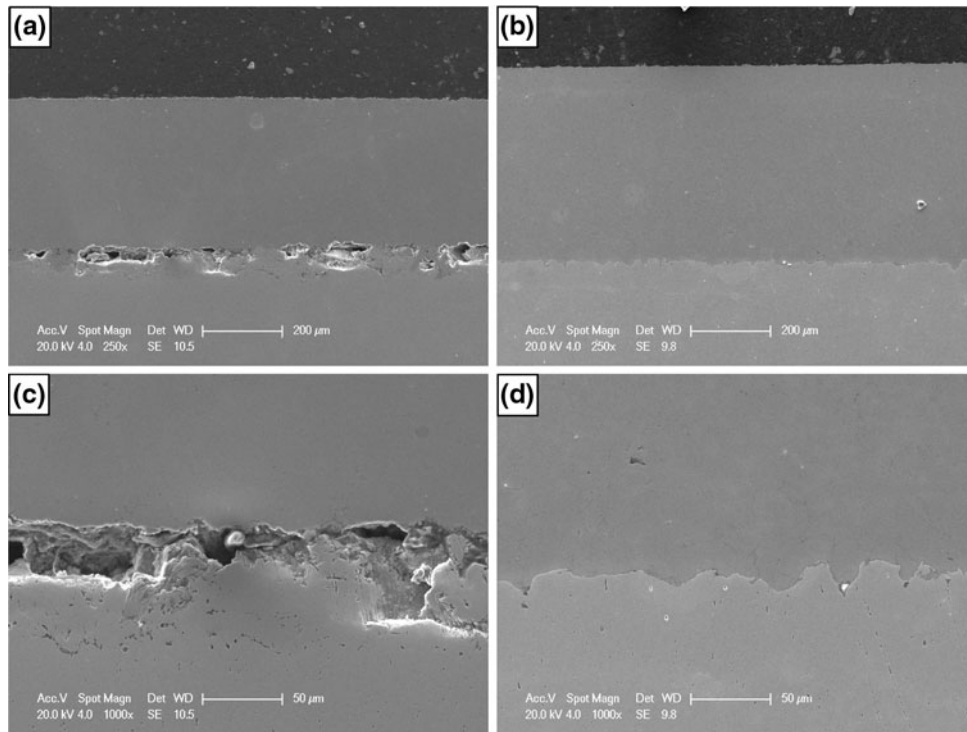| Specimens	OCP, mV[a]	E_{corr}, mV[a]	I_{corr}, mA/cm^2	I_{pp}, mA/cm^2
Bulk titanium	−285	−281	1×10^{-4}	0.004
As-sprayed coating (onto carbon steel)	−500	−507	5×10^{-3}	0.6
Laser-treated coating	−285	−294	5×10^{-5}	0.005
Carbon steel	−590	−567	2×10^{-2}	...

[a] wt. Ag/AgCl

Fig. 7 SE images of unetched coatings: (a) as-sprayed (onto carbon steel) and (b) laser-treated coatings after electrochemical tests. (c) and (d) are the corresponding high magnification images at the interface

Figure 7(a) and (b) show low-magnification cross sections of the as-sprayed coating and laser-treated coating, respectively, after the electrochemical tests in the aerated solution. It is evident that the coating-substrate interface of the as-sprayed sample has severe pitting following the electrochemical tests, whereas the laser-treated coating-substrate interface is free from any defect or pitting. Figure 7(c) and (d) show higher magnification images of the respective coating-substrate interfaces which confirm the severe pitting associated with the as-sprayed coating on carbon steel without the benefit of laser treatment.

4. Discussion

Following laser surface melting, the inter-particle porosity in the top 140 μm of the coating was eliminated. In the laser-treated zone, the rounded shape of the as-sprayed particles was also eliminated and an equiaxed grain structure formed on solidification and cooling to room temperature (Fig. 2). However, the etched microstructure of the coating showed a few isolated submicron-sized pores (Fig. 3b). These pores are probably trapped gas pores which are typical features in laser treated, thermal sprayed coatings. Titanium has a high melting temperature (1668 °C) and a high affinity for oxygen and nitrogen; it goes through an allotropic phase transformation at 882 °C, where hexagonally close packed (hcp) α-titanium transforms to body centered cubic (bcc) β-titanium. On solidification, bcc β-titanium is expected to form from the melt. Cooling in the solid state will give either hcp α-titanium or martensitic α-titanium (Ref 21). It is evident from Fig. 4 that hcp α-titanium has formed. Peak height ratios are as expected from a random, i.e., not preferentially oriented α-titanium grain structure. Presumably, columnar β-titanium formed but β- to α-titanium transition gives a random grain orientation. In addition,
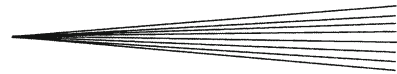
TiO was detected in XRD spectra of the laser-treated deposit and not TiO_2 (Fig. 4).

The laser posttreatment of the cold sprayed titanium coating eliminated the interconnected porosity near the surface (Fig. 2) and resulted in a shift of 215 mV in the OCP and E_{corr} values toward the noble direction and a decrease, by two orders of magnitude, of the I_{pp} value when compared to the as-sprayed condition. In addition, the OCP did not decrease over time but remained close to the level attained by bulk titanium. Hence, the resolidified top layer provides an impermeable barrier. However, its corrosion characteristics both in terms of OCP and anodic polarization are subtly different to that of bulk titanium. Although postspray laser treatment has been previously reported to improve the corrosion performance of plasma-sprayed titanium coatings (Ref 1, 16, 20, 22) further investigation is needed to understand the reasons for the differences in the behavior of bulk and laser-treated materials.

Typically, in the presence of an electrolyte at the coating-substrate interface, the carbon steel substrate, being less noble, corrodes and corrosion pits form at the coating-substrate interface; this is clearly seen with the titanium coating tested in the as-sprayed condition (Fig. 7a and c). The laser treatment applied following the spray deposition sealed completely the top 150 μm of the coating and pits are not visible as evidenced from Fig. 7(b) and (d); this occurred as a consequence of the formation of the melt pool and subsequent solidification which prevents corrosive species from penetrating the coating.

5. Conclusions

Titanium was deposited on carbon steel by cold spraying using nitrogen as a propelling gas. A number of laser trials were performed to eliminate the inter-connected porosity from the top layer of the coatings. The corrosion performance of the as-sprayed and postspray laser-treated coatings were studied in 3.5 wt.% NaCl solution. The following conclusions are drawn from the above study:

- Laser surface posttreatment of the cold sprayed titanium coating eliminates interconnected porosity in the top ~140 μm of the coatings without any deleterious effect on the substrate.
- The laser-treated titanium coating performs like a high-quality barrier layer and has corrosion values (i.e., OCP, E_{corr}, and I_{pp}) very close to those of bulk titanium.

Acknowledgments

References

1. T. Kinos, S.L. Chen, P. Siitonen, and P. Kettunen, Densification of Plasma Sprayed Titanium and Tantalum Coatings, *J. Therm. Spray Technol.*, 1996, **5**(4), p 439-444
2. P.A. Mäusli, Surface Characterisation of Titanium and Titanium alloys, *Adv. Biomater.*, 1986, **6**, p 57-62
3. R. Krepski, *Thermal Spray Coating Applications in the Chemical Process Industries*, M.T.I. Publication No. 42, NACE International, Georgetown, PA, 1993
4. D.M. Brunette, P. Tengvall et al., *Titanium in Medicine: Material Science, Surface Science, Engineering, Biological Responses and Medical Applications*, Springer, Berlin, London, 2001, p 376-415
5. E. Muehlberger, Method and Apparatus for Effecting High-Energy Dynamic Coating of Substrates, U.S. Patent No. 3,839,618, 1973
6. T. Schmidt, F. Gärtner, and H. Kreye, New Developments in Cold Spray Based on Higher Gas and Particle Temperatures, *J. Therm. Spray Technol.*, 2006, **15**(4), p 488-494
7. T. Marrocco, D.G. McCartney, P.H. Shipway, and A.J. Sturgeon, Production of Titanium Deposits by Cold-Gas Dynamic Spray: Numerical Modeling and Experimental Characterization, *J. Therm. Spray Technol.*, 2006, **15**(2), p 263-272
8. S.H. Zahiri, C.L. Antonio, and M. Jahedi, Elimination of Porosity in Directly Fabricated Titanium via Cold Gas Dynamic Spraying, *J. Mater. Process. Technol.*, 2009, **209**(2), p 922-929
9. H.R. Wang, B.R. Hou, J. Wang, Q. Wang, and W.Y. Li, Effect of Process Conditions on Microstructure and Corrosion Resistance of Cold-Sprayed Ti Coatings, *J. Therm. Spray Technol.*, 2008, **17**(5-6), p 736-741
10. D.L. Gilmore, R.C. Dykhuizen et al., Particle Velocity and Deposition Efficiency in the Cold Spray Process, *J. Therm. Spray Technol.*, 1999, **8**(4), p 576-582
11. W.-Y. Li and C.-J. Li, Deposition Characteristics of Titanium Coating in Cold Spraying, *Surf. Coat. Technol.*, 2003, **167**, p 278-283
12. T. Hussain, D.G. McCartney, P.H. Shipway, and T. Marrocco, Corrosion Behavior of Cold Sprayed Titanium Coatings and Free Standing Deposits, *J. Therm. Spray Technol.*, 2011, **20**(1-2), p 260-274
13. H.R. Wang, W.Y. Li, L. Ma, J. Wang, and Q. Wang, Corrosion Behavior of Cold Sprayed Titanium Protective Coating on 1Cr13 Substrate in Seawater, *Surf. Coat. Technol.*, 2007, **201**(9-11), p 5203-5206
14. W.-M. Zhao, C. Liu, L.-X. Dong, and Y. Wang, Effects of Arc Spray Process Parameters on Corrosion Resistance of Ti Coatings, *J. Therm. Spray Technol.*, 2009, **18**(4), p 702-707
15. K. Ishikawa, T. Suzuki, Y. Kitamura, and S. Tobe, Corrosion Resistance of Thermal Sprayed Titanium Coatings in Chloride Solution, *J. Therm. Spray Technol.*, 1999, **8**(2), p 273-278
16. T. Kinos, S.L. Chen, P. Siitonen, and P. Kettunen, Corrosion Properties of Shrouded Plasma Sprayed Titanium Coatings, *Thermal Spraying: Current Status and Future Trends*, A. Ohmori, Ed., High Temperature Society of Japan (Kobe, Japan), 1995, p 573-576
17. J. Kawakita, H. Katanoda, M. Watanabe, K. Yokoyama, and S. Kuroda, Warm Spraying: An Improved Spray Process to Deposit Novel Coatings, *Surf. Coat. Technol.*, 2008, **202**(18), p 4369-4373
18. W.M. Steen, *Laser Material Processing*, 3rd ed., Springer, Berlin, 2003
19. J.C. Ion, *Laser Processing of Engineering Materials: Principles, Procedure and Industrial Application*, Elsevier Butterworth-Heinemann, Amsterdam, 2005
20. H.D. Steffens, J. Wilden, and C. Buchmann, Laser Beam Nitriding of Thermally Sprayed Titanium Coatings, *Thermal Spraying: Current Status and Future Trends*, A. Ohmori, Ed., High Temperature Society of Japan (Kobe, Japan), 1995, p 981-986
21. P. Danielson, R. Wilson, and D. Alman, Microstructure of Titanium Welds, *Adv. Mater. Process.*, 2003, **161**(2), p 39-42
22. J.D. Ayers, R.J. Schaefer, F.D. Bogar, and E. McCafferty, Corrosion Behavior of Laser Consolidated Titanium Coated Steel in Sea-Water, *Corrosion*, 1981, **37**(1), p 55-57
23. N.D. Tomashov and P.M. Altovskii, Corrosion and Protection of Titanium, Government Scientific-Technical Publication of Machine-Building Literature (Russian Translation), Moscow, Russia, 1963